

Published in final edited form as:

IEEE Trans Ultrason Ferroelectr Freq Control. 2010 October ; 57(10): 2138–2146. doi:10.1109/TUFFC.2010.1670.

Relaxor-PT Single crystals: Observations and Developments

Shujun Zhang* and Thomas R. Shrout

Materials Research Institute, Pennsylvania State University, University Park, PA, 16802

Abstract

Relaxor-PT based ferroelectric single crystals $\text{Pb}(\text{Zn}_{1/3}\text{Nb}_{2/3})\text{O}_3\text{-PbTiO}_3$ (PZNT) and $\text{Pb}(\text{Mg}_{1/3}\text{Nb}_{2/3})\text{O}_3\text{-PbTiO}_3$ (PMNT) attracted lot of attentions in last decade due to their ultra high electromechanical coupling factors and piezoelectric coefficients. However, owing to a strongly curved morphotropic phase boundary (MPB), the usage temperature of these perovskite single crystals is limited by T_{RT} - the rhombohedral to tetragonal phase transition temperature, which occurs at significantly lower temperatures than the Curie temperature T_{C} . Furthermore, the low mechanical quality factors and coercive fields of these crystals, usually being on the order of ~ 70 and $2\text{--}3\text{ kV/cm}$, respectively, restrict their usage in high power applications. Thus, it is desirable to have high performance crystals with high temperature usage range and high power characteristics. In this survey, different binary and ternary crystal systems were explored, with respect to their temperature usage range, general trends of dielectric and piezoelectric properties of relaxor-PT crystal systems were discussed related to their $T_{\text{C}}/T_{\text{RT}}$. In addition, two approaches were proposed to improve mechanical Q values, including acceptor dopant strategy, analogous to “hard” polycrystalline ceramics, and anisotropic domain engineering configurations.

I. Introduction

Relaxor-based single crystals, such as $\text{Pb}(\text{Zn}_{1/3}\text{Nb}_{2/3})\text{O}_3\text{-PbTiO}_3$ (PZNT) and $\text{Pb}(\text{Mg}_{1/3}\text{Nb}_{2/3})\text{O}_3\text{-PbTiO}_3$ (PMNT), offer electromechanical coupling factors ($k_{33}^2 > 0.6$) and piezoelectric strain coefficients ($d_{33s} > 2000$ pC/N) that far out-perform the polycrystalline PZT based ceramics with couplings $k_{33}^2 \sim 0.5$ and piezoelectric $d_{33} \sim 400\text{--}600$ pC/N, as depicted in Fig. 1, making them promising candidates for medical ultrasonics, sonar transducers and solid-state actuators [1–15]. However, their relatively low Cure temperatures ($T_{\text{Cs}} \sim 130\text{--}170^\circ\text{C}$) may limit their application in transducers in which thermal stability is a pre-requirement in terms of dielectric and piezoelectric property variation and depolarization as a result of post-fabrication processes. Their implementation if further restricted by the T_{RT} - the ferroelectric rhombohedral to ferroelectric tetragonal phase transition, which occurs at a significantly lower temperature than the T_{C} , owing to strongly curved morphotropic phase boundaries (MPB) [8–10]. A generic phase diagram for relaxor-PT single crystals is shown in Fig. 2, depicting a strongly curved MPB, showing the $T_{\text{R-T}}$ is far below the Curie temperature, especially at the MPB composition, where the highest piezoelectric properties are expected. Thus, single crystal systems with a high Curie temperature for enhanced temperature usage range and thermal stability are desired.

In addition to thermal environments, ferroelectric crystals used in electromechanical devices, such as high power ultrasonic transducers or actuators, are subjected to high electric fields, which necessitate that the crystals possess low dielectric/mechanical losses and relatively high coercive fields. The dielectric loss of PMNT and PZNT crystals are reported to be on the order of $\leq 0.4\%$, similar to values observed in “hard” PZT based piezoelectrics,

*Corresponding author: soz1@psu.edu.

however, the mechanical quality factors (inverse of mechanical loss of crystals) were found to be only 10^2 , similar to “soft” PZT ceramics, limit crystals for high power transducer applications operating at resonance frequency [16–17]. Furthermore, the coercive fields (E_C) of crystals, being 2–3kV/cm, reflecting the depolarization electric field, will restrict the actuation applications under high dc drive, further limited by field induced ferroelectric phase transitions (E_{FF}). Therefore, it is important to explore why relaxor-PT single crystals possess low dielectric loss, yet exhibit high mechanical loss and low E_C/E_{FF} .

In this paper, we review recent works on the enhancements of both T_C and T_{RT} of relaxor-PT based crystal systems with expanded temperature usage range. A second focus of this review is the role of dopant and/or crystallographic domain engineering on the mechanical losses and their origin. Finally, general observations of the properties, with respect to their T_C/T_{RT} are made.

II. Relaxor-PT systems with high Curie temperature

Table I presents a list of several lead based relaxor-PT systems, including the $\text{Pb}(\text{Sc}_{1/2}\text{Nb}_{1/2})\text{O}_3\text{-PbTiO}_3$ (PSNT), $\text{Pb}(\text{In}_{1/2}\text{Nb}_{1/2})\text{O}_3\text{-PbTiO}_3$ (PINT) and $\text{Pb}(\text{Yb}_{1/2}\text{Nb}_{1/2})\text{O}_3\text{-PbTiO}_3$ (PYNT), which have been found to possess relatively high Curie temperatures near their MPB compositions [18–20]. Henceforth, numerous researchers have focused on single crystals of these binary systems and/or ternary systems with PMN [21–34].

PSNT single crystals with MPB composition(s) were successfully grown by the high temperature solution method, as reported by Yamashita et al. [21] and Bing et al. [22–23]. Crystals with compositions in the ternary systems $\text{Pb}(\text{Sc}_{1/2}\text{Nb}_{1/2})\text{O}_3\text{-Pb}(\text{Mg}_{1/3}\text{Nb}_{2/3})\text{O}_3\text{-PbTiO}_3$ (PSMNT)[24] and $\text{Pb}(\text{Sc}_{1/2}\text{Nb}_{1/2})\text{O}_3\text{-Pb}(\text{Zn}_{1/3}\text{Nb}_{2/3})\text{O}_3\text{-PbTiO}_3$ (PSZNT) [25] were also grown by the flux method or solution Bridgman method. To date, however, it has been difficult to grow PSNT based crystals directly from the melt due to the inadequate perovskite stability, thus limiting crystal growth to a few millimeters in dimension.

Single crystals in the PINT system were grown by the high temperature flux method and their electromechanical properties have been determined in last few years [26–28]. Single crystals in the binary PINT and ternary $\text{Pb}(\text{In}_{1/2}\text{Nb}_{1/2})\text{O}_3\text{-Pb}(\text{Mg}_{1/3}\text{Nb}_{2/3})\text{O}_3\text{-PbTiO}_3$ (PIMNT) [29] systems were also grown using the modified Bridgman techniques, with transition temperatures on the order of 200 °C and piezoelectric properties d_{33} of $\sim 2000\text{pC/N}$ reported, however, they exhibited a low ferroelectric phase transition, T_{R-T} , on the order of 80–110 °C, similar to the binary PMNT.

The MPB composition in PYNT system exhibited T_C of ~ 360 °C, the highest among all the lead based relaxor-PT systems (see Table I) and similar to PZT. Single crystals in the PYNT system were grown using the flux method [30–34], with Curie temperature T_C and the rhombohedral to tetragonal phase transition temperature T_{RT} observed to be 325°C and 160°C, respectively. The increased T_{RT} results in a broadened temperature usage range and also stabilizes the property temperature dependence as reported in ref. [32]. However, as found in the PSNT system, only small size crystals with few millimeters can be achieved.

Of particular interest are the new high Curie temperature bismuth based perovskite single crystals in $(1-x)\text{Bi}(\text{Me})\text{O}_3\text{-xPbTiO}_3$, specifically, the $\text{BiScO}_3\text{-PbTiO}_3$ (BSPT) system, where a Curie temperature around ~ 450 °C (100°C higher than the PZT materials) was observed for the MPB composition(s) ($x=0.64$). BSPT single crystals with different PT contents have been grown by flux method and characterized [35–39]. The T_C and T_{RT} were found to be on the order of 402°C and 349 °C for 0.43BS-0.57PT (BSPT57) single crystals [37], both much higher than that found for the lead based relaxor-PT systems, with comparable piezoelectric

properties. The temperature dependence of the piezoelectric and electromechanical properties of the rhombohedral BSPT57 were measured and found to exhibit temperature independent behavior till 330 °C, close to its T_{RT} . Furthermore, the BSPT57 crystals possessed high coercive field, being on the order of 13kV/cm [37]. Analogous to PSNT and PYNT systems, BSPT crystals have only been grown using high temperature flux method, limiting crystals to millimeter size.

In order to obtain relaxor-PT single crystals of sufficient size for commercial applications, two approaches have been used, including the modified Bridgman growth of PIN-PMN-PT/PMNT [40–44] and SSCG of PMN-PZT/PMNT [45–51] systems.

Recently, it was reported that ternary PIN-PMN-PT single crystal boules (>50mm in diameter and >100mm in length) can be grown directly from the melt by the modified Bridgman technique [13–14, 40–44], with Curie temperatures of >170°C, while maintaining piezoelectric properties comparable to binary PMNT crystals. Fig. 3 gives the phase diagram for the PIN-PMN-PT system, in which, single crystals with compositions of $PIN > 0.25$ – 0.35 , $PT > 0.30$ – 0.32 , have been grown and investigated [40–44]. Analogous to PMNT, the composition along the growth directions $\langle 001 \rangle / \langle 110 \rangle$ varies due to the segregation of Ti, Mg and In, being on the order of 7%, 5% and 2%, respectively. As found for PMNT, the lower PT content was at the bottom part of the crystal boule while the top of the boule was found to be in tetragonal phase. Common to all the relaxor-PT crystal systems, the rhombohedral to tetragonal phase transition observed in PIN-PMN-PT ternary crystals, occurs well below its Curie temperature due to the strongly curved MPB. As expected, T_{RT} of >120°C, 30°C higher than PMNT, can be achieved in the ternary PIN-PMN-PT system [43].

In addition to the modified Bridgman technique, the SSCG/templated grain growth method has been demonstrated to offer another route to obtain relaxor-PT single crystals [45–51]. PMNT crystals with 40mm in size have been successfully grown by SSCG method and the piezoelectric properties were found to be comparable to that of the Bridgman grown crystals [15, 50–51]. A key advantage of the SSCG technique is that no compositional segregation happens during the growth and crystals with uniform composition can be obtained. Single crystals in PMN-PZT ternary system was explored to further increase the T_C and T_{RT} . Fig. 4 shows the schematic phase diagram of PMN-PZT system, where the tetragonal phase area is bounded by a convex curve toward PT. MPB compositions lie on this curve, which separates tetragonal and rhombohedral/pseudo-cubic phase. Single crystals with compositions close to the MPB have been successfully grown, as shown in the circular region. Curie temperatures greater than 200°C, with T_{RT} s ranging from 95 to 170°C, have been achieved [46].

III. General relationship of the properties with T_C and T_{RT}

In polycrystalline ferroelectric materials, knowledge of the Curie temperature is an important parameter to establish temperature usage range and temperature dependent behavior, showing a strong relationship of dielectric and piezoelectric properties with T_C s, as shown in Fig. 1b. For relaxor-PT single crystals, however, both T_C and T_{RT} are key parameters, due to their strongly curved MPB, as shown in Fig. 2. Thus, it is desirable to understand the general relationship of the single crystal properties.

Fig. 5 shows the room temperature electromechanical coupling factor k_{33} , dielectric permittivity, piezoelectric coefficient d_{33} of relaxor-PT based ferroelectric single crystals as function of Curie temperature T_C or rhombohedral–tetragonal phase transition temperature T_{RT} . Fig. 5(a) gives the electromechanical k_{33} as function of Curie temperature for various crystal systems, where the k_{33} s were found to be on the order of 90% for all the $\langle 001 \rangle$ domain engineered rhombohedral relaxor-PT crystals, regardless of their T_{RT}/T_C . From Fig.

5(b) and (c), however, the dielectric permittivity and piezoelectric coefficient were found to decrease with increasing T_{RT} , and not T_C , as observed for polycrystalline ceramics (Fig. 1b).

IV. Recent developments of high T_C PIN-PMN-PT and PMN-PZT ternary crystals

Fig. 6 shows the main properties, including dielectric and electromechanical properties for PIN-PMN-PT and PMN-PZT crystals, compared to binary PMNT counterpart. For comparability, the compositions in these crystal systems were selected based on similar piezoelectric coefficient d_{33} , being in the range of 1500–1700pC/N. Fig. 6(a) gives the dielectric permittivity as a function of temperature for the crystals, in which, the Curie temperature were found to be 137, 185 and 216°C, with T_{RT} being on the order of 93, 128 and 145°C, for PMNT29, PIN-PMN-PT and PMN-PZT, respectively, in which, the T_C/T_{RT} temperatures were found to be the highest in PMN-PZT crystals [41,49]. The temperature coefficient of the dielectric permittivity was found to be $>5\%/^{\circ}\text{C}$ for PMNT crystals in the temperature range of 25–100°C, due to the low T_{RT} , while it was found to be 1.2% – 1.6%/°C in the same temperature range for PIN-PMN-PT and PMN-PZT crystals, revealing an improved temperature stability of dielectric behavior for the ternary crystals, due to their higher T_C/T_{RT} . Fig. 6(b) shows the temperature dependent electromechanical coupling variation ($\Delta k_{ij}/k_{ij}$), in which one can see that the electromechanical coupling drop at only 90°C for PMNT crystals, corresponding to its T_{RT} temperature, while the depolarization occur at 123°C and 140°C for PIN-PMN-PT and PMN-PZT crystals, respectively, indicating the high T_C/T_{RT} crystal systems possess broadened temperature usage range.

In addition to the thermal environments, ferroelectric crystals used in electromechanical devices are subjected to the combination of electric field/temperature/stress etc. Fig. 7(a) gives the phase diagram of the PMNT system as a function of dc bias [10]. It was observed that with increasing external dc bias, the T_C s of PMNT crystals increase while the T_{RT} s decrease, expanding the tetragonal phase, further limiting the usage temperature range for applications under external dc bias. This phenomenon happens because the spontaneous polarization for tetragonal crystals was along $\langle 001 \rangle$ direction, which will be stabilized when applied electric field was long $\langle 001 \rangle$ orientation. For comparison, Fig. 7(b) shows the temperature usage range of various crystal systems as function of dc bias, in which one can see that the ternary crystals show similar trend as that of PMNT with increasing dc bias, with usage range 30–40°C higher than PMNT.

V. General trends of “hard” ferroelectric materials

It is thought that “hard” ferroelectric materials possess higher coercive field E_C when compared to “soft” ones, however, in the same system, such as PZT, the E_C was found to be on the order of 12–18kV/cm

Fig. 8(d) presents the coercive fields (E_C) as function of T_C for different crystal systems, where the E_C was found to increase with increasing T_C . The E_C values were found to be on the order of 2–3kV/cm for PMNT/PZNT crystals with T_C being 140–170°C, while the coercive field for BSPT crystals was found to be 13kV/cm, five times higher than PMNT system, due to its higher Curie temperature, $\sim 405^{\circ}\text{C}$. It is interest to note that for the same crystal system, the tetragonal crystals were found to possess much higher coercive field when compared to its rhombohedral counterparts, being off the general trend as shown in Fig. 8(d), owing to the 90° domains in tetragonal phase were harder to be switched under applied fields, when compared to the $109^{\circ}/71^{\circ}$ domain walls in rhombohedral compositions.

It is hard to conclude what control the mechanical quality factor in ferroelectric materials: Curie temperature, coercive field and internal bias are closely related to the mechanical Q values. Fig. 9(a) shows mechanical Q as function of T_C for ferroelectric materials, including single crystals and polycrystalline ceramics. From a broad viewpoint, materials with higher T_C were found to possess higher mechanical Q . However, it was observed the Q values were scattered and random for the materials with T_C lower than 400°C . Fig. 9(b) gives the mechanical Q as function of internal bias in ferroelectric ceramics, it was found that the Q values increased with increasing the internal bias field, where “soft” ceramics were found to have low Q , being on the order of <100 , with no internal bias observed, while “hard” ceramics showing various internal biases and Q values, demonstrating that the internal bias plays an important role in the high Q ferroelectric ceramics. For single crystals, the scenario is more complicated, not only the internal bias affect the Q value, also the anisotropic domain structures should be considered.

VI. High power relaxor-PT single crystals

Relaxor-PT based ferroelectric single crystals have been reported to possess excellent properties in the $\langle 001 \rangle$ poled domain engineered state, with high piezoelectric coefficients $d_{33} > 1500 \text{ pC/N}$ and large electromechanical coupling factors $k_{33} > 0.9$, with low mechanical quality factor $Q \sim 120$. The combination of high piezoelectric properties and low Q make single crystals excellent components for non-resonant actuators and high frequency medical ultrasound transducers [16,17]. In contrast, however, the high power ultrasonic transducers generally use “hard” piezoelectric ceramics $\text{Pb}(\text{Zr},\text{Ti})\text{O}_3$ (PZT), including PZT4 and PZT8 (DOD Type I and III) [52]. These materials are characterized by low dielectric ($\tan\delta$) and mechanical losses (high mechanical quality factor Q). In general, to achieve the “hardening” effect, these materials are acceptor doped, resulting in the development of acceptor-oxygen vacancy defect dipoles. These dipoles align parallel to the polarization direction, leading to an internal bias, as evident in a horizontal offset in the polarization-electric field (P-E) behavior, clamping domain wall mobility [53,54]. A consequence of these dopants, however, is a reduction in electromechanical coupling and piezoelectric activity, so limits the bandwidth of transducer, since the power and bandwidth capabilities of the transducer are functions of the mechanical quality and electromechanical coupling factors [55]. Thus, the materials with both high electromechanical coupling and mechanical quality factor are desired.

Fig. 5(b) shows the polarization hysteresis for different crystal systems, from which, the coercive field can be obtained [41,49]. The coercive field was found to be 2.2 kV/cm for PMNT binary crystals, only half the values observed for the ternary crystals, being on the order of 4.5 kV/cm and 5.5 kV/cm for PMN-PZT and PIN-PMN-PT crystals, respectively. Fig. 5(c) presents the unipolar strain curves as a function of electric field, for different $\langle 001 \rangle$ domain engineered crystals, exhibiting low hysteresis characteristics [41,49]. The piezoelectric coefficients can be calculated from the slope of S-E curves at low electric field and found to be $1500\text{--}1700 \text{ pC/N}$ for all the crystals. Of particular interest is their different strain behavior, where the PMNT was found to possess three segments with different slopes, corresponding to the electric field induced rhombohedral to monoclinic and monoclinic to tetragonal phase transitions. It is desirable to keep the crystals in rhombohedral phase, where the threshold field was found to be 15 kV/cm for PMNT, above which, the crystal transformed to other phases and the property degraded, whereas this threshold electric field was found to be on the order of 55 kV/cm and 60 kV/cm for PMN-PZT and PIN-PMN-PT crystals, respectively, significantly increase the usage electric field range.

Based on the high piezoelectric properties of relaxor-PT single crystals, two approaches were proposed to further improve the mechanical Q values. Analogous to “hard” PZT

ceramics, the Mn acceptor dopant was investigated in PMN-PZT crystals, with enhanced mechanical Q (~ 1050) and low dielectric loss ($\sim 0.2\%$), while maintaining ultra high electromechanical coupling $k_{33} > 90\%$, inherent in $\langle 001 \rangle$ oriented domain engineered single crystals [16]. The effect of acceptor doping was also evident in the build-up of an internal bias ($E_i \sim 1.6\text{kV/cm}$), shown by a horizontal offset in the polarization-field behavior, as given in Fig. 7 [16]. It was also observed from Fig. 7 that the remnant polarization was reduced, while the coercive field increased in Mn-doped PMN-PZT crystals, demonstrating that the degree of “switchable” polarization is significantly reduced, owing to the domain wall clamping by the internal bias.

Different from PZT ceramics, there is no grain boundary in the single crystals, which show a strong anisotropic behavior. So it is important to explore the domain engineering configuration in the relaxor-PT crystals with different crystallographic orientations. It was found that the electrical and mechanical losses in crystals depends on the specific engineered domain configuration, with both high Q and high electromechanical coupling observed for the $\langle 110 \rangle$ oriented PMNT crystals [17]. Table II lists the longitudinal properties for pure and Mn-modified PIN-PMN-PT crystals along their primary crystallographic directions $\langle 001 \rangle$, $\langle 110 \rangle$ and $\langle 111 \rangle$, pure and Mn-doped PMN-PZT are also summarized in the table and compared to commercial “hard” PZT ceramics. It was found that the dielectric permittivity ϵ_r , dielectric loss ($\tan\delta = 1/Q_{\text{electric}}$), piezoelectric coefficient d_{33} and elastic compliance s_{33}^E reached the highest values for the $\langle 001 \rangle$ domain engineering configuration (4R) and exhibited minimum values for the $\langle 111 \rangle$ monodomain crystal (1R), with values for $\langle 110 \rangle$ poled samples (2R) lying in between. In contrast, the mechanical quality factor Q was maximum for the $\langle 111 \rangle$ oriented samples, being on the order of ~ 1000 , with values being less than ~ 160 for $\langle 001 \rangle$ oriented crystals. Of particular significance from Table II was the high mechanical Q , on the order of ~ 500 for the $\langle 110 \rangle$ engineered domain configuration, with an electromechanical coupling factor k_{33} on the order of ~ 0.91 . To delineate the anisotropic loss behavior, we must consider the role of domains in the relaxor-PT single crystals. As stated, there are two types of domains in rhombohedral relaxor-PT ferroelectric crystals, the 180° ferroelectric domains and non- 180° ferroelastic-ferroelectric domains (71° and 109° domains) [56–59]. The 180° domains refer to domain walls with antiparallel polarizations, but with strain tensors that are necessarily equivalent. Such domain walls will generally be moved by the application of an electric field [56], which only contribute to the polarization (dielectric loss). The non- 180° domain walls refer to walls between variants which differ in both polarization vector and strain tensor. Both 180° and non- 180° domain walls generally form to decrease the effects of depolarization fields, whereas only non- 180° domain walls may minimize the elastic energy. Thus, the dielectric and mechanical losses are originated from 180° and non- 180° domain wall motion, respectively [16, 60]. For $\langle 111 \rangle$ poled single crystals, the domain engineered structure is pseudo-monodomain “1R”, with no domain walls exist, thus, both low dielectric loss and high mechanical Q values are expected. Indeed, the dielectric loss was found to be only 0.1%, with a mechanical Q on the order of ~ 1000 for $\langle 111 \rangle$ poled PIN-PMN-PT. As stated above, the 180° domain walls in ferroelectric crystals can be moved by the application of electric field, accounting for the low dielectric loss in the relaxor-PT single crystals. However, four degenerated $109^\circ/71^\circ$ domain walls existed in $\langle 001 \rangle$ poled crystals, with engineered domain configuration 4R, which was found to be very stable under external electric field, however, large hysteresis was found when external stress applied along $\langle 001 \rangle$ direction, leading to large mechanical loss (low mechanical Q) in $\langle 001 \rangle$ direction. For $\langle 110 \rangle$ poled ferroelectric crystals with engineered domain configuration “2R”, only 71° domain existed, whereas 109° domains parallel to the (110) face, exhibiting much more stable domain structure when compared to “4R” engineered domain configuration, giving rise to a higher mechanical Q value in $\langle 110 \rangle$ poled polydomain PIN-PNN-PT crystals. Of particular interest is that no internal bias for $\langle 110 \rangle$ oriented crystals was observed,

demonstrating the high Q value of $\langle 110 \rangle$ orientation is attributed to anisotropic domain structure, other than internal bias, as found in acceptor doped ferroelectric materials.

Thus, the mechanical quality factors in relaxor-PT ferroelectric crystals can be improved by two approaches, either acceptor doping or anisotropic engineered domains. It is interesting to note that the combination of these two approaches will further enhance the mechanical Q . From Table I, $\langle 110 \rangle$ oriented Mn-doped PIN-PMN-PT crystals were found to possess higher coercive field and internal bias when compared to the pure counterpart, due to the domain wall clamping by the acceptor dopant, further increase the Q value along crystallographic $\langle 110 \rangle$ direction as expected.

As mentioned above, high electromechanical coupling factor k_{ij} and mechanical quality factor Q are desired for high power, broad bandwidth transducer applications. However, previous investigations have shown that both Q and k_{ij} can be enhanced only at the expense of each other in ferroelectric ceramics, as shown in Fig. 10, where it was observed that with increasing mechanical Q values, the electromechanical coupling decreased in PZT ceramics. Of particular significance is that for domain engineered relaxor-PT single crystal systems, either acceptor modification or $\langle 110 \rangle$ orientation can be used to improve the mechanical Q values, meanwhile maintaining ultra high electromechanical coupling, being on the order of 0.9.

V. Conclusion

In summary, relaxor-PT based single crystals, such as PMNT and PZNT, were extensively studied for actuation and transduction applications. However, their low temperature usage range (low T_{RT}), low coercive field and mechanical quality factor, limit their high power applications. In this study, ternary PIN-PMN-PT and PMN-PZT were investigated in details. The T_C of these two systems were found to be $>170^\circ\text{C}$, with T_{RT} being on the order of $120\text{--}150^\circ\text{C}$, significantly increase their usage temperature range by $30\text{--}60^\circ\text{C}$, when compared to commercial available PMNT crystals. The coercive fields were found to be on the order of 5 kV/cm , with electric field induced ferroelectric phase transition occurring at $50\text{--}60\text{ kV/cm}$ for $\langle 001 \rangle$ oriented crystals, due to their higher Curie temperature, expanding their field usage range greatly. Furthermore, the mechanical Q values were found to be increased, being on the order of 1000, by acceptor dopant and/or $\langle 110 \rangle$ engineered domain configuration, while maintaining the high electromechanical coupling factor ~ 0.9 . At last, the general trends of properties related to T_C/T_{RT} in relaxor-PT based ferroelectric single crystals were discussed. The dielectric permittivities and piezoelectric coefficients were found to decrease with increasing T_{RT} , while the coercive field was found to depend on the T_C . Of particular interest is the electromechanical couplings were found to be independent of T_C/T_{RT} , maintaining on the same order of 0.9, inherent in domain engineering single crystals.

Acknowledgments

The authors wish to thank Dr. Jun Luo and Dr. Wesley Hackenberger from TRS Technologies, Dr. Ho-Yong Lee from Ceracomp Co. Ltd. and Dr. Richard J. Meyer Jr, Nevin P. Sherlock from ARL, Penn State. The work was supported by NIH under Grant No. P41-EB21820 and ONR.

References

1. Park S, Shrout T. Characteristics of relaxor-based piezoelectric single crystals for ultrasonic transducers. *IEEE Trans Ultrason, Ferroelect, Freq Contr.* 1997; 44:1140–1147.
2. Park SE, Shrout TR. Ultrahigh strain and piezoelectric behavior in relaxor based ferroelectric single crystals. *J Appl Phys.* 1997; 82:1804–1811.

3. Saitoh S, Takeuchi T, Kobayashi T, Harada K, Shimanuki S, Yamashita Y. An improved phased array ultrasonic probe using $\text{Pb}(\text{Zn}_{1/3}\text{Nb}_{2/3})\text{O}_3\text{-PbTiO}_3$ single crystal. *Jpn J Appl Phys.* 1999; 38:3380–3384.
4. Zhang SJ, Lebrun L, Liu SF, Rhee S, Randall CA, Shrout TR. Piezoelectric shear coefficients of $\text{Pb}(\text{Zn}_{1/3}\text{Nb}_{2/3})\text{O}_3\text{-PbTiO}_3$ single crystals. *Jpn J Appl Phys.* 2002; 41:L1099–1102.
5. Luo HS, Xu GS, Xu HQ, Wang PC, Yin ZW. Compositional homogeneity and electrical properties of lead magnesium niobate titanate single crystals grown by a modified Bridgman technique. *Jpn J Appl Phys.* 2000; 39:5581–5585.
6. Zhang SJ, Lebrun L, Jeong DY, Randall CA, Zhang QM, Shrout TR. Growth and characterization of Fe-doped $\text{Pb}(\text{Zn}_{1/3}\text{Nb}_{2/3})\text{O}_3\text{-PbTiO}_3$ single crystals. *J Appl Phys.* 2003; 93:9257–9262.
7. Zhang R, Jiang B, Jiang WH, Cao WW. Anisotropy in domain engineered $0.92\text{Pb}(\text{Zn}_{1/3}\text{Nb}_{2/3})\text{O}_3\text{-}0.08\text{PbTiO}_3$ single crystal and analysis of its property fluctuations. *IEEE Trans Ultrason Ferro Freq Cont.* 2002; 49:1622–7.
8. Davis M, Damjanovic D, Setter N. Electric-field, temperature, and stress-induced phase transitions in relaxor ferroelectric single crystals. *Phys Rev B.* 2006; 73:014115.
9. Zhang SJ, Luo J, Xia R, Rehrig PW, Randall CA, Shrout TR. Field-induced piezoelectric response in $\text{Pb}(\text{Mg}_{1/3}\text{Nb}_{2/3})\text{O}_3\text{-PbTiO}_3$ single crystals. *Solid State Communications.* 2006; 137 :16–20.
10. Zhang, S.J.; Luo, J.; Shanta, R.; Snyder, D.; Shrout, TR. ‘Modified $\text{Pb}(\text{Mg}_{1/3}\text{Nb}_{2/3})\text{O}_3\text{-PbTiO}_3$ single crystals for high temperature application. Proceedings of 15th IEEE-ISAF, NC; Sunset beach. 2006. p. 261-264.
11. Zhou QF, Wu D, Jin J, Hu CH, Xu X, Williams J, Cannata J, Lim LC, Shung KK. Design and fabrication of PZN-7%PT single crystal high frequency angled needle ultrasound transducers. *IEEE Trans Ultrason Ferro Freq Contr.* 2008; 55:1394–1399.
12. Zhou QF, Xu X, Gottlieb E, Sun L, Cannata J, Ameri H, Humayun M, Han PD, Shung KK. PMN-PT single crystal high frequency ultrasonic needle transducers for pulsed wave doppler application. *IEEE Trans Ultrason Ferro Freq Contr.* 2007; 54:668–675.
13. <http://www.trstechnologies.com>
14. <http://www.hcmat.com>
15. <http://ceracomp.com/>
16. Zhang SJ, Lee SM, Kim DH, Lee HY, Shrout TR. Characterization of Mn-modified $\text{Pb}(\text{Mg}_{1/3}\text{Nb}_{2/3})\text{O}_3\text{-PbZrO}_3\text{-PbTiO}_3$ single crystals for high power broad bandwidth transducers. *Appl Phys Lett.* 2008; 93:122908. [PubMed: 19529783]
17. Zhang SJ, Sherlock NP, Meyer RJ Jr, Shrout TR. Crystallographic dependence of loss in domain engineered relaxor-PT single crystals. *Appl Phys Lett.* 2009; 94:162906. [PubMed: 19654880]
18. Yamashita Y. Large electromechanical coupling factors in perovskite binary material system. *Jpn J Appl Phys.* 1994; 33:5328–31.
19. Landolt-Bornstein. *Ferroelectrics and Related Substances.* Vol. 16. Berlin, Heidelberg, NY: Springer-Verlag; 1981.
20. Zhang, S.J.; Luo, J.; Snyder, DW.; Shrout, TR. High performance, high T_C piezoelectric crystals. In: Ye, ZG., editor. *Handbook of advanced dielectric, piezoelectric and ferroelectric materials.* CRC Press; NY: 2008. p. 130-157.
21. Yamashita Y, Harada K. Crystal growth and electrical properties of lead scandium niobate lead titanate binary single crystals. *Jpn J Appl Phys.* 1997; 36:6039–42.
22. Bing YH, Ye ZG. Effects of chemical compositions on the growth of relaxor ferroelectric $\text{Pb}(\text{Sc}_{1/2}\text{Nb}_{1/2})\text{O}_3\text{-PbTiO}_3$ single crystals. *J Cryst Growth.* 2003; 250:118–25.
23. Bing YH, Ye ZG. Synthesis, phase segregation and properties of piezo-/ferroelectric $\text{Pb}(\text{Sc}_{1/2}\text{Nb}_{1/2})\text{O}_3\text{-PbTiO}_3$ single crystals. *J Cryst Growth.* 2006; 287:326–9.
24. Hosono Y, Harada K, Yamashita Y, Dong M, Ye ZG. Growth, electric and thermal properties of lead scandium niobate-lead magnesium niobate-lead titanate ternary single crystals. *Jpn J Appl Phys.* 2000; 39:5589–92.
25. Ichinose N, Saigo Y, Hosono Y, Yamashita Y. Preparation and dielectric properties of high T_C relaxor-based single crystals. *Ferroelectrics.* 2002; 267:311–6.

26. Guo Y, Luo HS, He T, Yin Z. Peculiar properties of a high Curie temperature $\text{Pb}(\text{In}_{1/2}\text{Nb}_{1/2})\text{O}_3\text{-PbTiO}_3$ single crystal grown by the modified Bridgman technique. *Solid Stat Commun.* 2002; 123:417–20.
27. Yasuda N, Ohwa H, Hasegawa D, Hayashi K, Hosono Y, Yamashita Y, Iwata M, Ishibashi Y. Temperature dependence of piezoelectric properties of a high Curie temperature $\text{Pb}(\text{In}_{1/2}\text{Nb}_{1/2})\text{O}_3\text{-PbTiO}_3$ binary system single crystal near a morphotropic phase boundary. *Jpn J Appl Phys.* 2000; 39:5586–8.
28. Duan ZQ, Xu GS, Wang XF, Yang DF, Pan XM, Wang PC. Electrical properties of high Curie temperature $(1-x)\text{Pb}(\text{In}_{1/2}\text{Nb}_{1/2})\text{O}_3\text{-xPbTiO}_3$ single crystals grown by the solution Bridgman technique. *Sol Stat Commun.* 2005; 134:559–63.
29. Hosono Y, Yamashita Y, Sakamoto H, Ichinose N. Large piezoelectric constant of high Curie temperature $\text{Pb}(\text{In}_{1/2}\text{Nb}_{1/2})\text{O}_3\text{-Pb}(\text{Mg}_{1/3}\text{Nb}_{2/3})\text{O}_3\text{-PbTiO}_3$ ternary single crystal near morphotropic phase boundary. *Jpn J Appl Phys.* 2002; 41:L1240–2.
30. Yasuda N, Ohwa H, Kume M, Hosono Y, Yamashita Y, Ishino S, Terauchi H, Iwata M, Ishibashi Y. Crystal growth and dielectric properties of solid solutions of $\text{Pb}(\text{Yb}_{1/2}\text{Nb}_{1/2})\text{O}_3\text{-PbTiO}_3$ with a high Curie temperature near a morphotropic phase boundary. *Jpn J Appl Phys.* 2001; 40:5664–7.
31. Zhang SJ, Rehrig PW, Randall CA, Shrout TR. Crystal growth and electrical properties of $\text{Pb}(\text{Yb}_{1/2}\text{Nb}_{1/2})\text{O}_3\text{-PbTiO}_3$ perovskite single crystals. *J Crys Growth.* 2002; 234:415–20.
32. Zhang SJ, Priya S, Furman E, Shrout TR, Randall CA. A random-field model for polarization reversal in $\text{Pb}(\text{Yb}_{1/2}\text{Nb}_{1/2})\text{O}_3\text{-PbTiO}_3$ single crystals. *J Appl Phys.* 2002; 91:6002–6.
33. Zhang SJ, Rhee S, Randall CA, Shrout TR. Dielectric and piezoelectric properties of high Curie temperature single crystals in the $\text{Pb}(\text{Yb}_{1/2}\text{Nb}_{1/2})\text{O}_3\text{-PbTiO}_3$ solid solution series. *Jpn J Appl Phys.* 2002; 41:722–6.
34. Zhang SJ, Lebrun L, Rhee S, Randall CA, Shrout TR. Shear mode piezoelectric properties of $\text{Pb}(\text{Yb}_{1/2}\text{Nb}_{1/2})\text{O}_3\text{-PbTiO}_3$ single crystals. *Appl Phys Lett.* 2002; 81:892–4.
35. Zhang SJ, Lebrun L, Rhee S, Eitel RE, Randall CA, Shrout TR. Crystal growth and characterization of new high Curie temperature $(1-x)\text{BiScO}_3\text{-PbTiO}_3$ single crystals. *Crystal Grow.* 2002; 236:210–216.
36. Zhang SJ, Jeong DY, Zhang QM, Shrout TR. Electromechanical and electro-optic properties of $x\text{BiScO}_3\text{-yBiGaO}_3\text{-(1-x-y)PbTiO}_3$ single crystals. *Crystal Grow.* 2003; 247:131–136.
37. Zhang SJ, Randall CA, Shrout TR. High Curie Temperature Piezocrystals in the $\text{BiScO}_3\text{-PbTiO}_3$ Perovskite System. *Appl Phys Lett.* 2003; 83:3150–3152.
38. Zhang SJ, Randall CA, Shrout TR. Characterization of perovskite piezoelectric single crystals of $0.43\text{BiScO}_3\text{-}0.57\text{PbTiO}_3$ with high Curie temperature. *J Appl Phys.* 2004; 95:4291–5.
39. Zhang SJ, Randall CA, Shrout TR. Recent developments in high Curie temperature perovskite single crystals. *IEEE Trans Ultrason Ferro Freq Cont.* 2005; 52:564–9.
40. Xu GS, Chen K, Yang DF, Li JB. Growth and electrical properties of large size PIN-PMN-PT crystals prepared by the vertical Bridgman technique. *Appl Phys Lett.* 2007; 90:032901.
41. Zhang SJ, Luo J, Hackenberger W, Shrout TR. Characterization of PIN-PMN-PT ferroelectric crystal with enhanced phase transition temperatures. *Appl Phys.* 2008; 104:064106.
42. Tian J, Han PD, Huang XL, Pan HX. Improved stability for piezoelectric crystals grown in the lead indium niobate-lead magnesium niobate-lead titanate system. *Appl Phys Lett.* 2007; 91:222903.
43. Zhang SJ, Luo J, Hackenberger W, Sherlock NP, Meyer RJ Jr, Shrout TR. Electromechanical characterization of PIN-PMN-PT crystals as a function of crystallographic orientation and temperature. *Appl Phys.* 2009; 105:104506.
44. Liu XZ, Zhang SJ, Luo J, Shrout TR, Cao WW. Complete set of material constants of PIN-PMN-PT single crystal with morphotropic phase boundary composition. *Appl Phys.* 2009; 106:074112.
45. Zhang SJ, Lee SM, Kim DH, Lee HY, Shrout TR. Characterization of high T_C PMN-PZ-PT single crystals fabricated by solid state crystal growth. *Appl Phys Lett.* 2007; 90:232911.
46. Zhang SJ, Lee SM, Kim DH, Lee HY, Shrout TR. Electromechanical properties of PMN-PZT piezoelectric single crystals near morphotropic phase boundary compositions. *Am Ceram Soc.* 2007; 90:3859–3862.
47. Amin A, Lee HY, Kelly B. High transition temperature lead magnesium niobate-lead zirconate titanate single crystals. *Appl Phys Lett.* 2007; 90:242912.

48. Messing GL, Trolier-Mckinstry S, Sabolsky EM, Duran C, Kwon S, Brahmroutu B, Park P, Yilmaz H, Rehrig PW, Eitel KB, Suvaci E, Seabaugh M, Oh KS. Templated grain growth of textured piezoelectric ceramics. *Critical Rev Sol Stat Mater Sci.* 2004; 29:45–96.
49. Zhang SJ, Lee SM, Kim DH, Lee HY, Shrout TR. Temperature dependence of the dielectric, piezoelectric and elastic constants for PMN-PZ-PT piezocrystals. *Appl Phys.* 2007; 102:114103.
50. Lee, HY. Development of high performance piezoelectric single crystals by using solid-state single crystal growth (SSCG) method. In: Ye, ZG., editor. *Handbook of advanced dielectric, piezoelectric and ferroelectric materials.* CRC Press; NY: 2008. p. 158-172.
51. Zhang SJ, Lee SM, Kim DH, Lee HY, Shrout TR. Elastic, piezoelectric and dielectric properties of 0.71PMN-0.29PT crystals obtained by solid-state crystal growth. *Am Ceram Soc.* 2008; 91:683–686.
52. Pohanka, RC.; Smith, PL. Chapter 2- Recent advances in piezoelectric ceramics. In: Levinson, LM., editor. *Electronic Ceramics- Properties, Devices and Applications.* NY: 1987.
53. Carl K, Hardtl KH. Electrical after-effects in PZT ceramics. *Ferroelectrics.* 1978; 17:473–486.
54. Takahashi S. Effects of impurity doping in lead zirconate-titanate ceramics. *Ferroelectrics.* 1982; 41:143–156.
55. Meyer, RJ.; Montgomery, TC.; Hughes, WJ. Tonpiz transducers designed using single crystal piezoelectrics. *Oceans '02 MTS/IEEE Proceeding; Mississippi.* October 29–31, 2002; 2002. p. 2328-2333.
56. Davis, M. PhD Thesis. *Ceramics Laboratory, Swiss Federal Institute of Technology; 2006.* Phase transitions, anisotropy and domain engineering: the piezoelectric properties of relaxor-ferroelectric single crystals.
57. Bokov AA, Ye ZG. Domain structure in monoclinic Pm phase of PMN-PT single crystals. *J Appl Phys.* 2004; 95:6347–6359.
58. Han JP, Cao WW. Interweaving domain configurations in [001] poled rhombohedral phase PMN-PT single crystals. *Appl Phys Lett.* 2003; 83:2040–2.
59. Davis M, Damjanovic D, Hayem D, Setter N. Domain engineering of the transverse piezoelectric coefficient in perovskite ferroelectrics. *Appl Phys.* 2005; 98:014102.
60. Uchino K, Zheng J, Chen YH, Du XH, Ryu J, Gao Y, Ural S, Priya S, Hirose S. Loss mechanisms and high power piezoelectrics. *J Mater Sci.* 2006; 41:217–28.

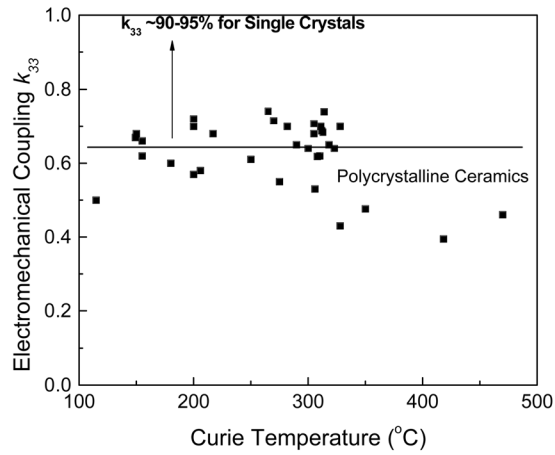


Fig. 1 (a)

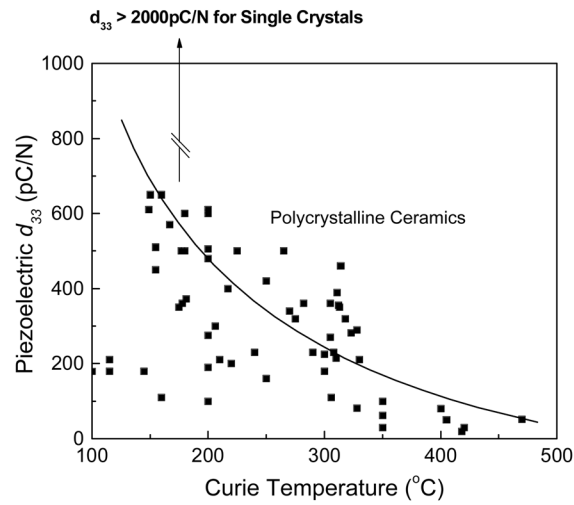


Fig. 1(b)

Fig. 1. Electromechanical coupling k_{33} and piezoelectric d_{33} of Relaxor-PT single crystals, compared to polycrystalline piezoelectric ceramics as a function of Curie temperature, the crystal systems exhibit significantly higher values (after [20]).

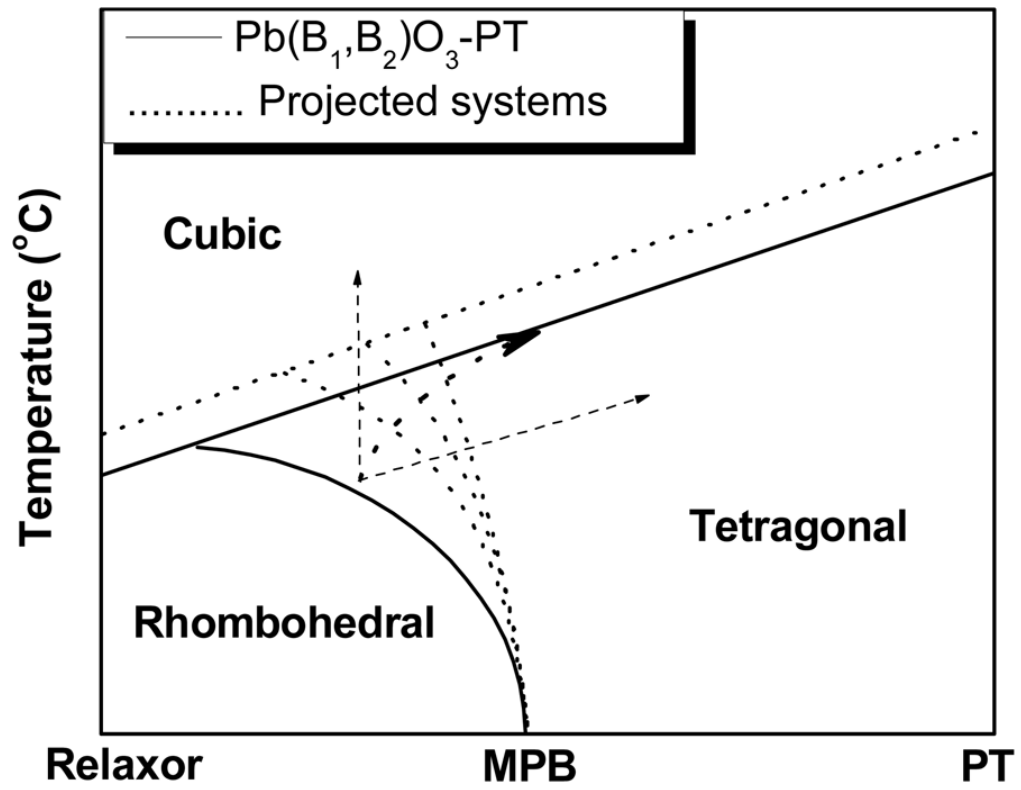


Fig. 2. A generic phase diagram for relaxor-PT crystal systems, depicting a strongly curved MPB, the dotted line is the projected phase diagram for modified systems (after [20]).

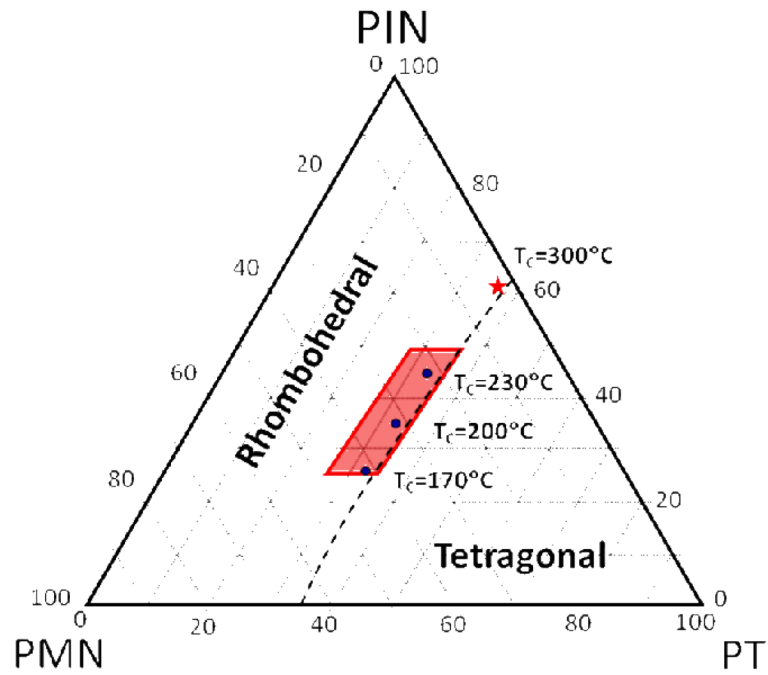


Fig. 3.
Schematic phase diagram for PIN-PMN-PT ternary system.

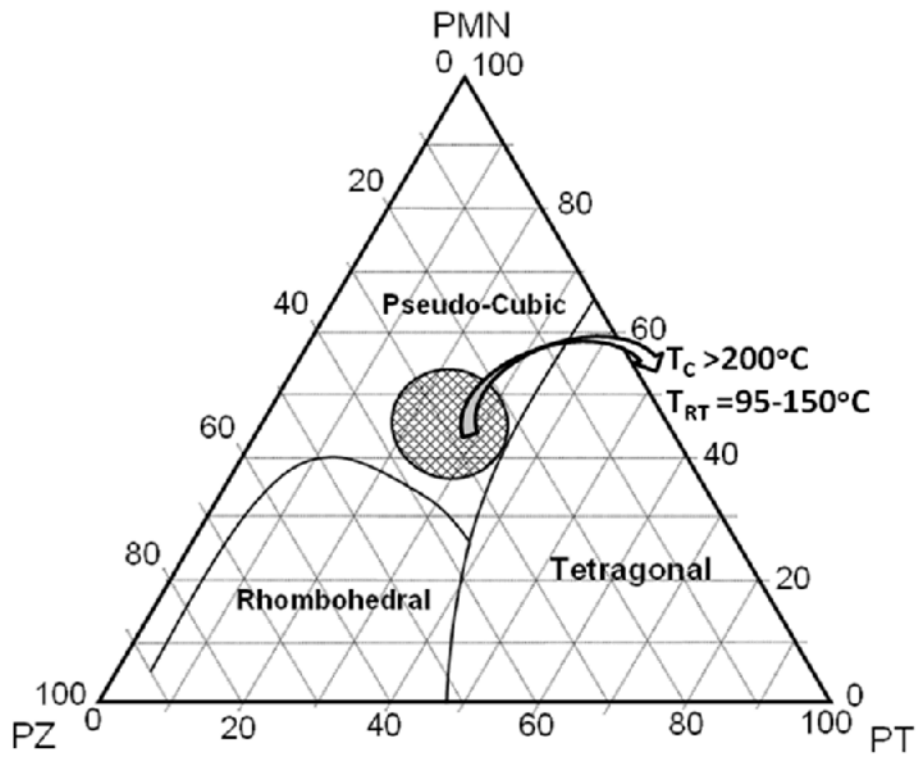


Fig. 4. Schematic phase diagram for PMN-PZT ternary system (after [46]).

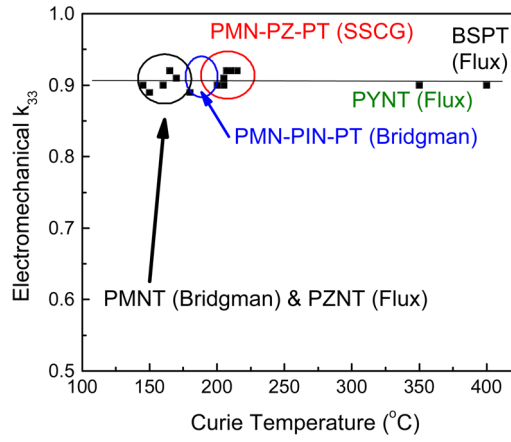


Fig. 5 (a)

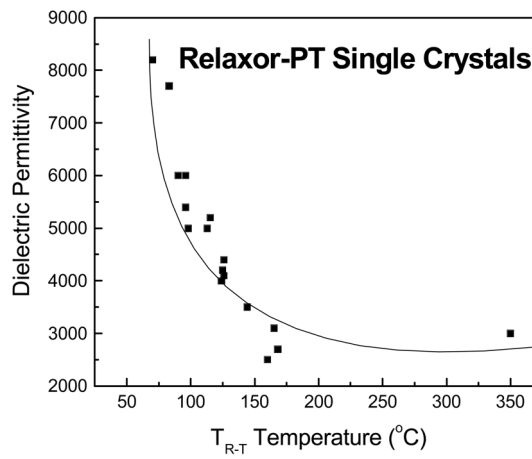


Fig. 5 (b)

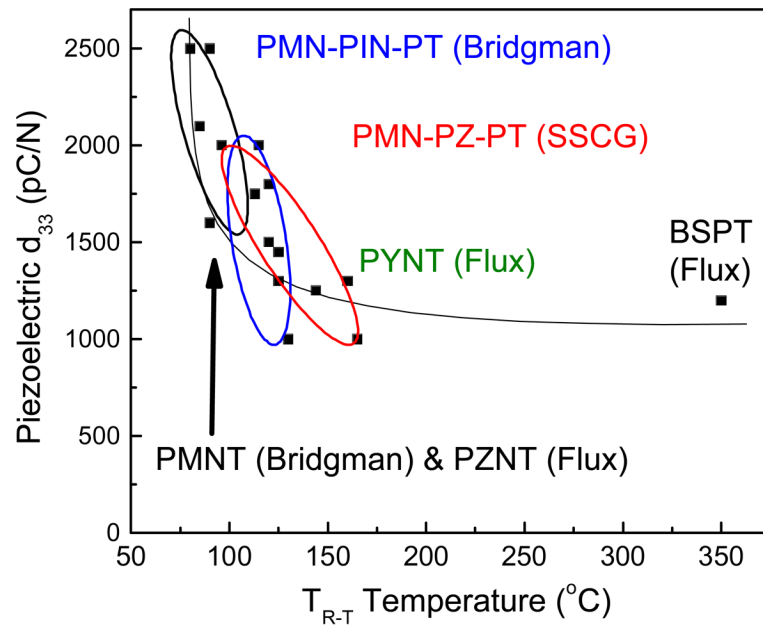


Fig. 5 (c)

Fig. 5. (a) Electromechanical coupling k_{33} as function of T_C ; (b) Dielectric permittivity as function of T_{RT} ; (c) Piezoelectric coefficient d_{33} as function of T_{RT} for various relaxor-PT crystal systems (data obtained from references [1–51]).

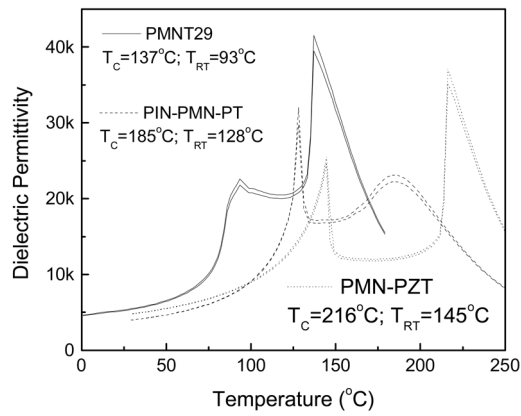


Fig. 6 (a)

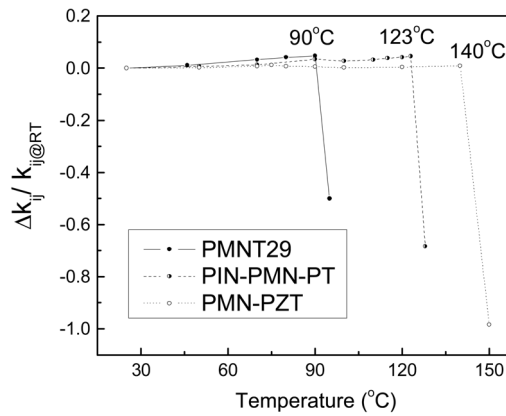


Fig. 6 (b)

Fig. 6. (a) Dielectric permittivity as function of temperature; (b) Bipolar polarization hysteresis; (c) Unipolar strain as function of electric field; (d) Electromechanical coupling variation as function of temperature for PIN-PMN-PT and PMN-PZT crystals, compared to PMNT.

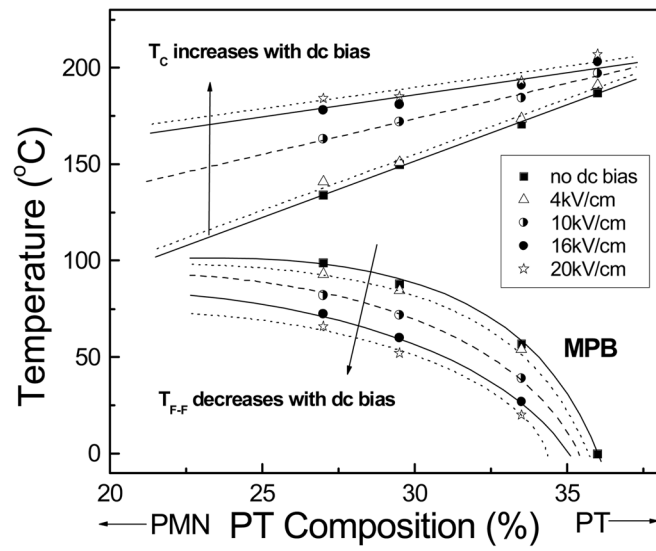


Fig. 7 (a)

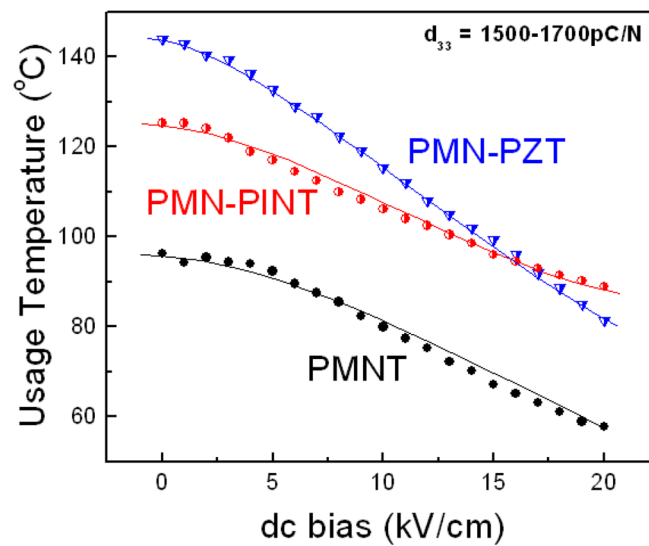


Fig. 7(b)

Fig. 7. (a) Phase diagram for PMNT single crystals under different dc bias fields (after [10]), (b) Temperature usage range for PIN-PMN-PT and PMN-PZT ternary systems, compared to PMNT crystals.

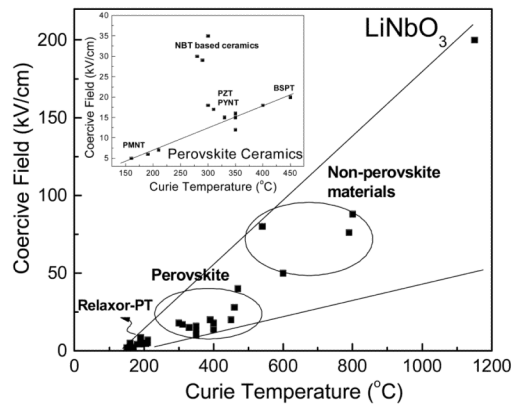


Fig. 8 (a)

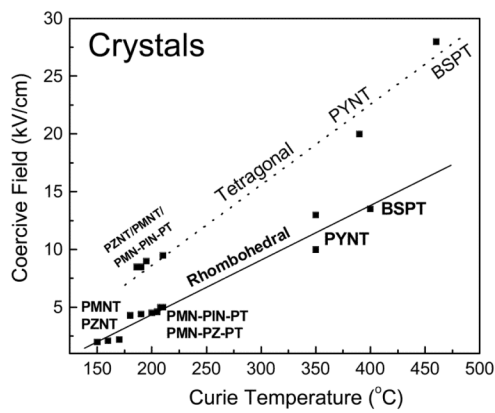


Fig. 8 (b)

Fig. 8. Bipolar polarization hysteresis of pure and Mn modified PMN-PZT single crystals (after [16]).

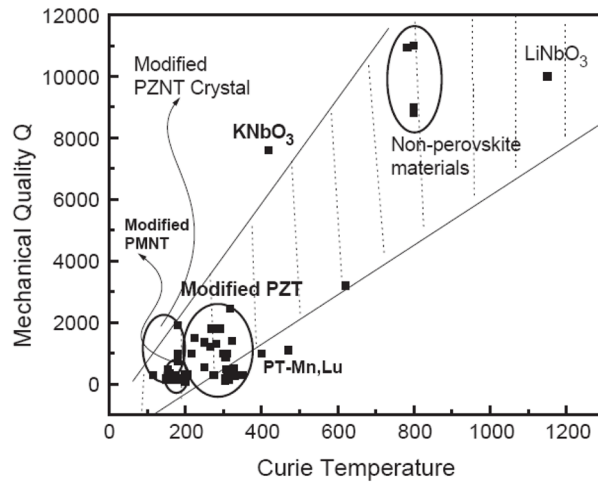


Fig. 9 (a)

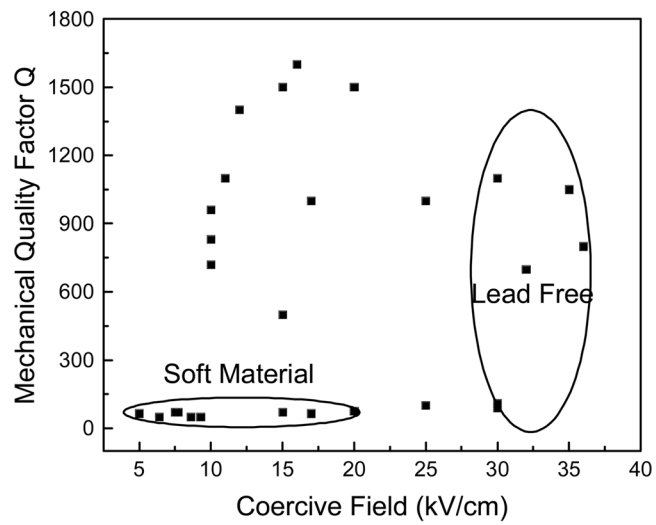


Fig. 9 (b)

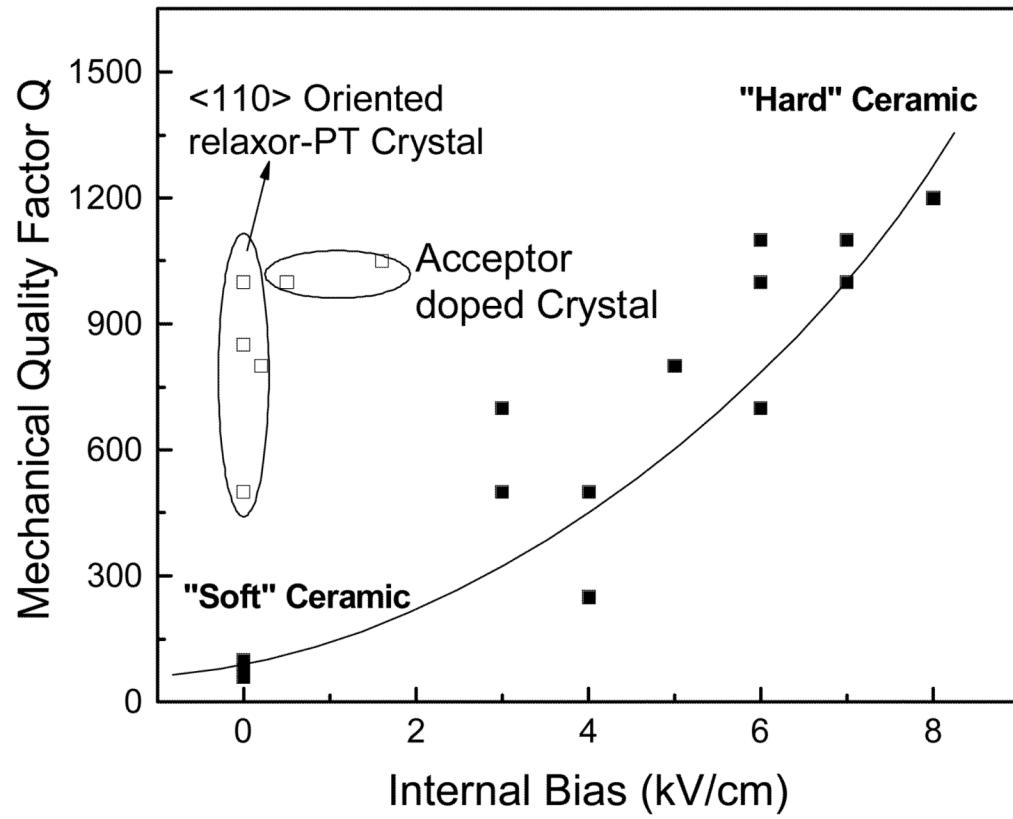


Fig. 9 (c)

Fig. 9.

(a) Mechanical quality factor as function of Curie temperature for different materials; (b) Mechanical quality factor as function of internal bias for ferroelectric ceramics.

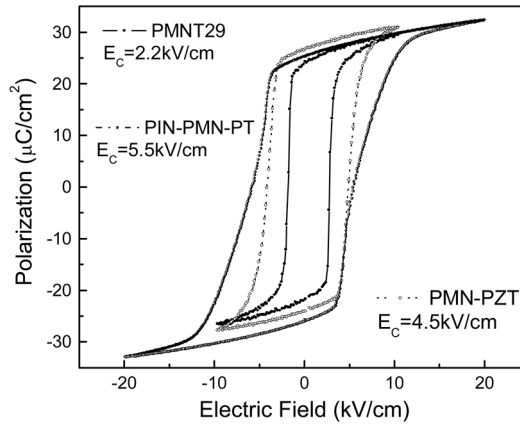


Fig. 10 (a)

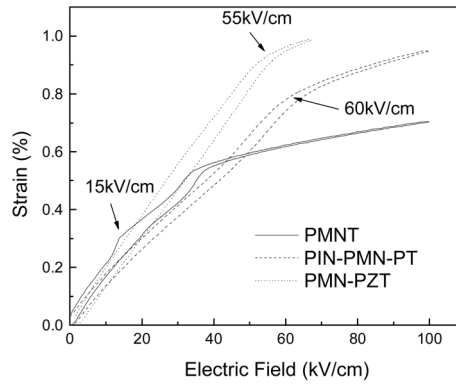


Fig. 10 (b)

Fig. 10. The relationship between mechanical quality factor Q and electromechanical coupling factor k_{33} , for different polycrystalline and single crystal systems.

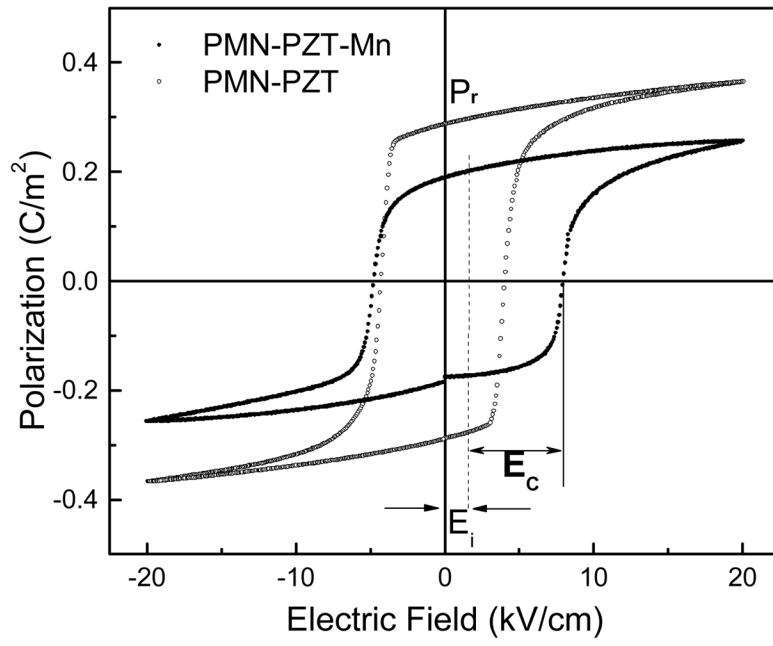


Fig. 11.

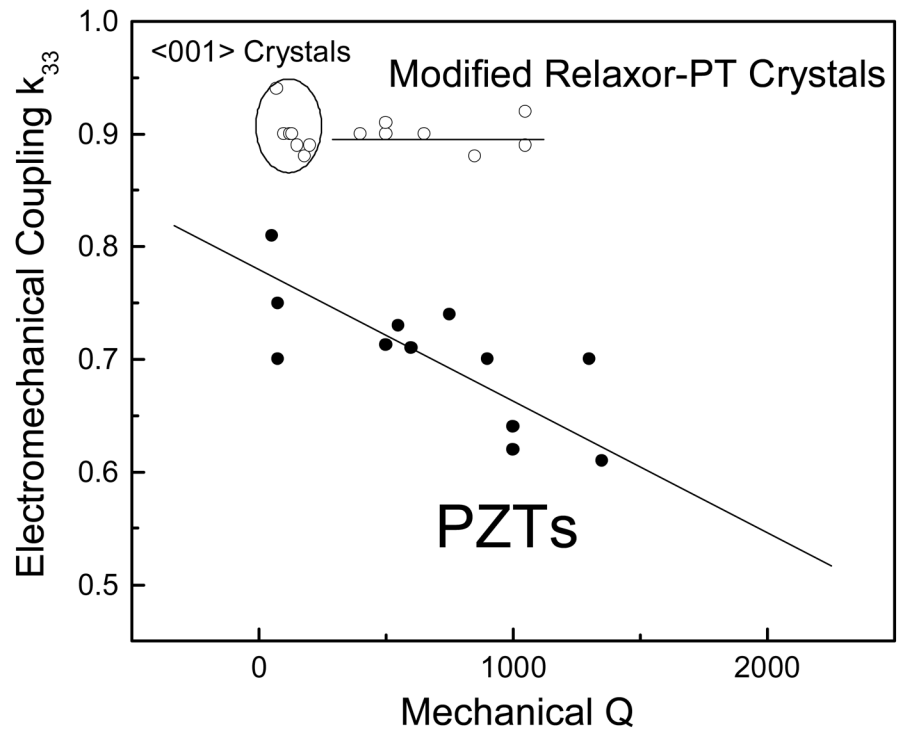


Fig. 12.

Table IMorphotropic Phase Boundaries in Perovskite $\text{Pb}(\text{B}_1\text{B}_{\text{II}})\text{O}_3$ -PT Systems.

Binary System	PT content on MPB	T_C (°C) at MPB	T_{R-T} (°C) at MPB
(1-x) $\text{Pb}(\text{Zn}_{1/3}\text{Nb}_{2/3})\text{O}_3$ -x PbTiO_3 (PZNT)	$x \cong 0.09$	~180	95
(1-x) $\text{Pb}(\text{Mg}_{1/3}\text{Nb}_{2/3})\text{O}_3$ -x PbTiO_3 (PMNT)	$x \cong 0.33$	~150	80
(1-x) $\text{Pb}(\text{Ni}_{1/3}\text{Nb}_{2/3})\text{O}_3$ -x PbTiO_3 (PNNT)	$x \cong 0.40$	~130	/
(1-x) $\text{Pb}(\text{Co}_{1/3}\text{Nb}_{2/3})\text{O}_3$ -x PbTiO_3 (PCNT)	$x \cong 0.38$	~250	/
(1-x) $\text{Pb}(\text{Sc}_{1/2}\text{Nb}_{1/2})\text{O}_3$ -x PbTiO_3 (PSNT)	$x \cong 0.43$	~260	100
(1-x) $\text{Pb}(\text{Sc}_{1/2}\text{Ta}_{1/2})\text{O}_3$ -x PbTiO_3 (PSTT)	$x \cong 0.45$	~205	/
(1-x) $\text{Pb}(\text{Fe}_{1/2}\text{Nb}_{1/2})\text{O}_3$ -x PbTiO_3 (PFNT)	$x \cong 0.07$	~140	/
(1-x) $\text{Pb}(\text{In}_{1/2}\text{Nb}_{1/2})\text{O}_3$ -x PbTiO_3 (PINT)	$x \cong 0.37$	~320	120
(1-x) $\text{Pb}(\text{Yb}_{1/2}\text{Nb}_{1/2})\text{O}_3$ -x PbTiO_3 (PYNT)	$x \cong 0.50$	~360	160
(1-x) $\text{Pb}(\text{Mg}_{1/2}\text{W}_{1/2})\text{O}_3$ -x PbTiO_3 (PMWPT)	$x \cong 0.55$	~60	/
(1-x) $\text{Pb}(\text{Co}_{1/2}\text{W}_{1/2})\text{O}_3$ -x PbTiO_3 (PCWPT)	$x \cong 0.45$	~310	/

Table II

Longitudinal properties for pure and Mn –modified PIN-PMN-PT crystals with different orientations, compared to PMN-PZT crystals and PZT ceramics.

Material	E_c/E_{int} (kV/cm)	ϵ_r	Loss (%)	k_{33}	d_{33} (pC/N)	s_{33}^E (pm ² /N)	Q_{33}
PIN-PMN-PT	<001>	4400	0.4	0.92	1500	68.0	160
	<110>	3400	0.2	0.91	925	34.8	500
	<111>	700	0.1	0.36	74	6.8	1000
Mn-PIN-PMN- PT	<001>	3600	0.4	0.90	1200	55.8	800
	<110>	3000	0.4	0.89	900	38.5	1050
PMN-PZT	<001>	4850	0.5	0.93	1530	63.1	100
Mn-PMN-PZT	<001>	3410	0.2	0.92	1140	50.9	1050
PZT4	/	1300	0.4	0.70	300	15.5	500
PZT8	/	1000	0.4	0.64	230	13.5	1000